Annals of Microbiology (2019) 69:713–726
https://doi.org/10.1007/s13213-019-01463-w

ORIGINAL ARTICLE

The effect of pitching rate on the production of higher alcohols by top-fermenting yeast in wheat beer fermentation

Mengqi Wang[1] · Zhongguan Sun[1] · Yaping Wang[1] · Zhiyang Wei[1] · Bingxu Chen[1] · Huadong Zhang[1] · Xuewu Guo[1,2] · Dongguang Xiao[1,2]

Received: 1 September 2018 / Accepted: 13 March 2019 / Published online: 26 March 2019

Abstract

Purpose The level of higher alcohols on top-fermentation determines the flavor profile and is one of the most important elements dictating the favorable top-fermented wheat beer (Ale beer) development. The optimization of the pitching rate has been shown to be crucial for industrial beer brewing. This study focused on understanding the effect of the variable inoculum size on the synthesis of higher alcohols.

Methods We utilized sequencing to investigate the transcript changes under different inoculum sizes and link the results to fermentation performance.

Results Variable cell inoculum density levels were linked with differences in higher alcohol production. Specifically, we observed significantly less higher alcohols produced at lower cell inoculum density during the stationary phase. Importantly, the accumulation of higher alcohols during the exponential growth phase was overall similar between different pitching rates. Moreover, free amino nitrogen (FAN) consumption and yeast cell viability were significantly decreased during stationary phase at the lowest inoculum density. Transcriptomic analysis revealed that amino acid metabolism genes *ALD4*, *ALD6*, *ARO9*, *ARO10*, and *PUT1* were differentially expressed once the cells entered the declining growth phase at the lowest inoculum size.

Conclusion The results suggest that the variable accumulation of higher alcohols in the top-fermenting yeast at different inoculum sizes is mostly accounted for in the stationary phase. We discovered that lower pitching rate was associated with a negative effect on amino acid metabolism and synthesis of higher alcohols during the stationary phase, leading to the decrease in higher alcohol concentration at low inoculum densities. Overall, our study provides valuable insights that could benefit wheat beer production.

Keywords Top-fermenting · Higher alcohols · Pitching rate · Stationary phase · Cell viability · Amino acid metabolism

Introduction

Higher alcohols, also known as fusel alcohols, are one of the most abundant and important elements determining the flavor profile of beer (Pires et al. 2014). These volatile compounds produced by yeast during the fermentation of wort can produce undesirable flavor when their concentrations exceed certain threshold values (Kobayashi et al. 2014). Examples of higher alcohols include n-propanol (sweet aroma), isobutanol (solvent-like aroma), isoamylol (banana-like aroma), active amyl alcohol (solvent-like aroma), and 2-phenylethanol (rose-like aroma) (Meilgaard 1975; Engan 1981; Landaud et al. 2001; Meilgaard 2001). The major higher alcohols are produced via two pathways: the anabolic pathway (Harris) that catalyzes glucose through intermediates (α-keto acid) and the catabolic (Ehrlich) pathway which uses branched-chain amino acids (valine, leucine, isoleucine) and aromatic amino acids (phenylalanine) (Chen 1978; Hammond 1993).

During beer production, it is important to assure that the active substances contributing to beer flavor are kept within certain limits as modifications to one or more compounds can directly affect the flavor profile and cause deleterious health effects to humans (Saerens et al. 2008). The optimum concentration of higher alcohols in 12.0°P beers brewed by bottom

✉ Xuewu Guo
guoxuewu@tust.edu.cn

✉ Dongguang Xiao
xdg@tust.edu.cn

[1] Key Laboratory of Industrial Fermentation Microbiology, Ministry of Education, Tianjin Industrial Microbiology Key Lab, College of Biotechnology, Tianjin University of Science and Technology, Tianjin 300457, China

[2] Tianjin Engineering Research Center of Microbial Metabolism and Fermentation Process ControlChina, Tianjin 300457, China

fermentation is 70–120 mg/L. The concentration of higher alcohols is about 50 mg/L in barley beer with light taste and low malt content (Procopio et al. 2011; Pires et al. 2014). Top-fermented wheat beers, with their typically high fermentation temperatures of 20–24 °C and protein rich raw materials, contain a high concentration of higher alcohols (Vanderhaegen et al. 2003), which generate incompatible flavors and inhibit the development of wheat beer. Therefore, the development of effective methods aimed at decreasing the level of higher alcohols in wheat beer, particularly through the use of top-fermenting industrial brewer's yeast, is of great importance to both the consumers and the manufacturers (Zhang et al. 2013).

Optimization of the fermentation process and modification of parameters such as inoculum size, fermentation temperature, and substrate composition results in a significant variation in fermentation performance (Procopio et al. 2011). The pitching rate is one of the most important factors that influence the industrial beer brewing, and affects fermentation time, lag phase, the maximum biomass, and concentration of flavor-active substances (Sen and Swaminathan 2004). The volumetric productivity of the wheat beer fermentation process can be improved by optimizing the initial number of yeast cells in batch fermentation during industrial production (Okabe et al. 1992; Verbelen et al. 2008). For example, the higher inoculum sizes have been linked with deleterious effects on the flavor profile and can also negatively affect yeast cell physiology (Verbelen et al. 2009). In contrast, other studies have found that decreasing the initial cell concentration may have a positive effect on the industry production cost and the inheritance stability of yeast strain.

Despite many studies evaluating the impact of inoculum density on fermentation performance, the results remain inconclusive and the differences can be likely attributed to the use of different yeast strains. For example, studies by Verbelen et al. suggested that the free amino nitrogen (FAN) uptake level and concentrations of fusel alcohols were higher at higher inoculum sizes with lager yeast strain, even though the net yeast growth at different inoculum densities was constant (Verbelen et al. 2008). Moreover, other studies found that increased levels of certain esters, higher alcohols, and hop compounds were associated with decreasing pitching rate (Edelen et al. 1996). Interestingly, work by Carrau et al. revealed that there were significant changes in the concentration of esters, higher alcohols, and fatty acids on wine fermentation at three different inoculum levels; the results of the study were not immediately straightforward (Carrau et al. 2010). Finally, Erten et al. found that the levels of esters were constant using a lager yeast, while the concentration of higher alcohols significantly decreased with increasing pitching rates (Erten et al. 2007). However, so far, there are few studies focusing on effect of pitching rate on the production of higher alcohols by top-fermenting yeast in wheat beer fermentation.

In this study, the effect of pitching rate on wheat beer fermentation and production of higher alcohols was studied using a top-fermenting industrial brewer's yeast to investigate the impact of low pitching rates on the level of higher alcohols and wheat beer quality.

Materials and methods

Strains and medium

The experiments were performed using a wild-type top-fermenting industrial brewer's yeast, S-17, obtained from the Yeast Collection Center of the Tianjin Key Laboratory of Industrial Microbiology, Tianjin University of Science and Technology, China.

The yeast strain was grown at 30 °C in yeast extract peptone dextrose (YEPD) medium (1% yeast extract, 2% peptone, and 2% glucose). All solid media contained 2% agar (Difco, USA). Sterile all-wheat malt-hopped wort with 12 Plato (°P; g extract/100 g wort) (15% glucose, 60% maltose, 25% maltotriose, and 280 mg/L free amino nitrogen content) and without the addition of syrups was used in this study.

Fermentation conditions and sampling

A total of three different inoculum sizes were tested in the study: (Avbelj et al. 2015) 0.1% *v*/*v*, 5×10^5 cells/mL; (Bevers and Verachtert 1976) 1% *v*/*v*, 5×10^6 cells/mL; and (Chen et al. 2004) 10% *v*/*v*, 5×10^7 cells/mL. The fermentations were carried out under microaerophilic conditions in 5-L glass bottles (with 3 L of 12°P wort) sealed with rubber stoppers with a CO_2 outlet. Yeast strain was propagated in 1-L glass bottles (with 400 mL of 12°P wort) sealed with layers of gauze at 24 °C for 36 h under static conditions. Next, the yeast were inoculated into 5-L fermentation bottles following a brief spin (4000 rpm, 2 min), and washed three times with sterile water.

The fermentations were performed at 20 °C and were monitored every 8 h by withdrawing samples through a tubular liquid sampler. All samples were cooled directly on ice. The yeast cells and fermented wort were separated by centrifugation (4000 rpm, 2 min, 4 °C).

Fermentation analysis

Biomass of yeast cells was calculated from the absorbance measured at 600 nm, and the standard curve was generated using the dry weight of yeast. The specific gravity of the fermenting media was measured with a portable digital Brix refractometer (LH-B55, Lphand Biological, Hangzhou, China), and the extract content was measured with Alcoholyser Plus (Anton Paar, Graz, Austria). Gas

chromatography was used to determine the concentration of higher alcohols in the wort during the fermentation process and after the distillation as reported previously (Ma et al. 2017). The concentration of FAN was measured using a ninhydrin-based method, according to the standard method defined by the European Brewery Convention (1998).

Acidification power test

The samples were centrifuged (4000 rpm, 2 min, 4 °C) and washed three times with deionized water. The resulting pellet (4 g) was resuspended in 50 mL of deionized water in a 250-mL glass beaker, pH was adjusted to 6.3 with 0.01 M NaOH, and the samples were shaken at a speed of 100 rpm at 25 °C. Changes in pH were monitored every minute during the first 20 min. After 10 min, 5 mL of 20.2% *v*/*v* glucose solution (pH = 6.3) was added and two parameters were assessed. Specifically, we determined acidification power $(AP)_{10}$, the pH value at 10 min after the start of the measurement and AP_{20}, and the pH value at 20 min following the start of the measurement.

RNA extraction, library construction, and sequencing

The cells at the declining growth phase at different pitching rates were separated from wort by centrifugation (1341×*g*, 5 min), immediately frozen in liquid nitrogen, and shipped to the sequencing company on dry ice. The total RNA from each sample was extracted using RNeasy Mini Kits (Qiagen, Valencia, USA), and the RNA quantity and quality were assessed using an Agilent 2100 Bioanalyzer (Agilent Technologies, Palo Alto, CA, USA), NanoDrop (Thermo Fisher Scientific Inc.), and 1% agrose gel. Total RNA (1 μg) with an RNA Integrity Numbervalue above 7 was used for library preparation. Next-generation sequencing library preparations were constructed according to the manufacturer's protocol (NEBNext® Ultra™ RNA Library Prep Kit for Illumina®). Isolation of ploy(A) mRNA was performed using NEBNext Poly(A) mRNA Magnetic Isolation Module (NEB). The mRNA fragmentation and priming were performed by NEBNext First-Strand Synthesis Reaction Buffer and NEBNext Random Primers, respectively. The first-strand and second-strand cDNAs were synthesized using ProtoScript II Reverse Transcriptase and Second Strand Synthesis Enzyme Mix, respectively. The double-stranded cDNA was cleaned up using AxyPrep Mag polymerase chain reaction (PCR) Clean-up (Axygen, Corning, NY, USA), treated with End Prep Enzyme Mix for DNA end repair and dA-tailing in a single reaction, and then subjected to T-A ligation to add adaptors on both ends. Size selection of adaptor-ligated DNA was performed using AxyPrep Mag PCR Clean-up (Axygen), and fragments of ~360 bp (with the approximate insert size of 300 bp) were recovered. Each sample was amplified by PCR for 11 cycles using P5 and P7 primers containing adapter sequences that allow for annealing with the flow cell to perform bridge PCR and P7 with a six-base index that allows for multiplexing. The PCR products were cleaned using AxyPrep Mag PCR Clean-up Kit (Axygen), purity was confirmed using an Agilent 2100 Bioanalyzer (Agilent Technologies, Palo Alto, CA, USA), and the quantification was performed using Qubit 2.0 Fluorometer (Invitrogen, Carlsbad, CA, USA).Finally, the libraries with different indices were multiplexed and loaded onto Illumina HiSeq instrument according to the manufacturer's protocol (Illumina, San Diego, CA, USA). Sequencing was carried out using a 2 × 150-bp paired-end configuration. Image analysis and base calling were conducted by the HiSeq Control Software (HCS) + OLB + GAPipeline-1.6 (Illumina) on the HiSeq instrument.

Data quality control, mapping, and differential expression analysis

Pass filter data in FASTQ format were processed by Trimmomatic (v0.30) to remove technical sequences, such as adapters, PCR primers or fragments, and quality of bases lower than 20, to yield high-quality clean data of high quality.Hisat2 (v2.0.14) was used to index *S. cerevisiae* S288c genome sequence (NCBI; http://www.ncbi.nlm.nih.gov/), and the cleaned data were then aligned to the reference genome via Hisat2 software (v2.0.14) (Kim et al. 2015). Transcripts in fasta format were converted from a known GFF annotation file and appropriately indexed. Next, the HTSeq (v0.6.1) estimated the gene and isoform expression levels using the pair-end cleaned data. Differential expression analysis was performed using DESeq Bioconductor package, which is based on the negative binomial distribution. The Benjamini Hochberg approach was used to control for the false discovery rate (FDR), and a threshold of $P < 0.05$ was set to identify differentially expressed genes.

Kyoto Encyclopedia of Genes and Genomes enrichment analysis

Differentially expressed genes identified in our study were analyzed using in-house scripts to identify specifically enriched pathways in the Kyoto Encyclopedia of Genes and Genomes (KEGG) database (https://www.genome.jp/kegg/).

Kinetics and model simulation

The kinetics of microorganism growth can be fitted using many models, the most common of which are Monod growth model (resource-limited growth) and logistic growth model (space-limited growth) (Wang et al. 2015). The Monod growth model is not appropriate during the initial adaptation

phase when cells are diluted into a new culture (Kumar et al. 2014). Importantly, we observed an inhibition of cell growth mediated by the increase in cell density. Considering these results, the logistic growth model, which can well reflect the inhibiting effect of increased cell concentration on cell growth (Huang et al. 2014), was selected to fit the growth curve of top-fermenting yeast in wheat beer fermentation. The logistic equation was derived as follows:

$$ux = um\left(1-\frac{Cx}{Cm}\right) \tag{1}$$

where u_m is the maximum specific growth rate (h^{-1}), C_x is biomass (g/L), C_m is the maximum biomass (g/L), and t is the fermentation time (h).

After multiplying both sides by C_x, Eq. (1) could be changed as follows:

$$\frac{dCx}{dt} = um\left(1-\frac{Cx}{Cm}\right)Cx \tag{2}$$

At the beginning of fermentation, when $t = 0$, the $C_x = C_0$ (the initial biomass, g/L). Following an integral transform of Eq. (2), the kinetic model can be depicted as follows:

$$Cx = \frac{C0Cme^{umt}}{Cm-C0+C0e^{umt}} \tag{3}$$

It is commonly assumed that the higher alcohol production is closely related to the yeast cell growth and biomass accumulation. In this study, we used the Luedeking-Piret equation to describe the higher alcohol production at different inoculum sizes (Luedeking and Piret 1959):

$$\frac{dPx}{dt} = \alpha\frac{dCx}{dt} + \beta Cx \tag{4}$$

where P_x is the concentration of higher alcohols (mg/L), α is the growth-associated constant, β is the non-growth associated constant, and t is the fermentation time (h). When $\alpha \neq 0$, and $\beta = 0$, the product synthesis is directly related to cell growth; when $\alpha \neq 0$, and $\beta \neq 0$, the product synthesis is partially linked with cell growth; and when $\alpha = 0$, and $\beta \neq 0$, the product synthesis is not related to cell growth.

After integral transform, Eq. (4) could be changed as follows:

$$Px = \alpha\left(\frac{C0Cme^{umt}}{Cm-C0+C0e^{umt}}-C0\right)+\beta\left[\frac{Cm}{um}\ln\left(\frac{Cm-C0+C0e^{umt}}{Cm}\right)\right]+P0 \tag{5}$$

where P_0 is the initial concentration of higher alcohols (mg/L).

Model simulation and data fitting were performed using the OriginPro software (v9.0.0; OriginLab, Northampon, MA, USA). Model parameters are described in the text.

Results

Fermentation characteristics at three different inoculum sizes

The progress of the fermentations at different inoculum sizes is depicted in Fig. 1. In agreement with the initial assumptions, the speed of fermentation decreased with decreasing pitching rate. Importantly, we did not observe any significant differences in the real degree of fermentation (Rdf) among different inoculum densities. The time required to reach the constant Rdf (approximately 66%) was 96 h for the lowest pitching rate (0.1% *v/v*, 5×10^5 cells/mL); 88 h for the inoculum size of 1% *v/v*, 5×10^6 cells/mL; and 72 h for the normal inoculum density (10% *v/v*, 5×10^7 cells/mL). The level of sugar consumption was consistent with the findings about Rdf results. The final residual sugar concentration was not significantly correlated with the inoculum size, while the consumption rate of total sugar showed a decreasing trend with decreasing pitching rates.

Cell growth of the top-fermenting yeast S-17 at different inoculum densities (10% *v/v*, 1% *v/v*, 0.1% *v/v*) was monitored during the entire process of wheat beer fermentation (Fig. 1). Unsurprisingly, the stationary phase of growth was delayed for 24 h in sample with the lowest pitching rates, resulting in extended fermentation times at decreasing pitching rates. The maximum yeast cell biomass was lower in samples with lower inoculum size. Importantly, the net growth of the yeast cells, calculated by subtracting the initial cell number from the maximum cell number per unit of volume, was not significantly different at different inoculum sizes (10% *v/v*: 5.18 g/L, 1% *v/v*: 5.10229 g/L, 0.1% *v/v*: 5.11963 g/L). These data suggest that yeast growth was self-inhibited by the increase in cell concentration commonly observed in wheat beer batch fermentation, and we also observed that there is an obvious long lag time at the lowest pitching rate.

Kinetics of yeast cell growth

Data in Table 1 include parameters that were estimated from the experimental data using OriginPro (v9.0.0) software.

Overall, we observed that the logistic growth model was a great fit for the experimental data, with the correlation coefficient (*R*-square) values of 0.98923, 0.98784, and 0.98797 at 0.1% *v/v*, 1% *v/v*, and 10% *v/v* inoculum sizes, These results suggest that the logistic nonlinear fitting was suitable for predicting the growth of top-fermenting yeast S-17 in wheat beer fermentation. In addition, there were no significant differences in u_m, the maximum specific yeast growth rate, at varying pitching rates (10% *v/v*: 0.17273 h^{-1}, 1% *v/v*: 0.16949 h^{-1}, 0.1% *v/v*: 0.17252 h^{-1}) with decreasing pitching rates. The results suggest that the inoculum density is likely not associated with yeast cell proliferation rate during the

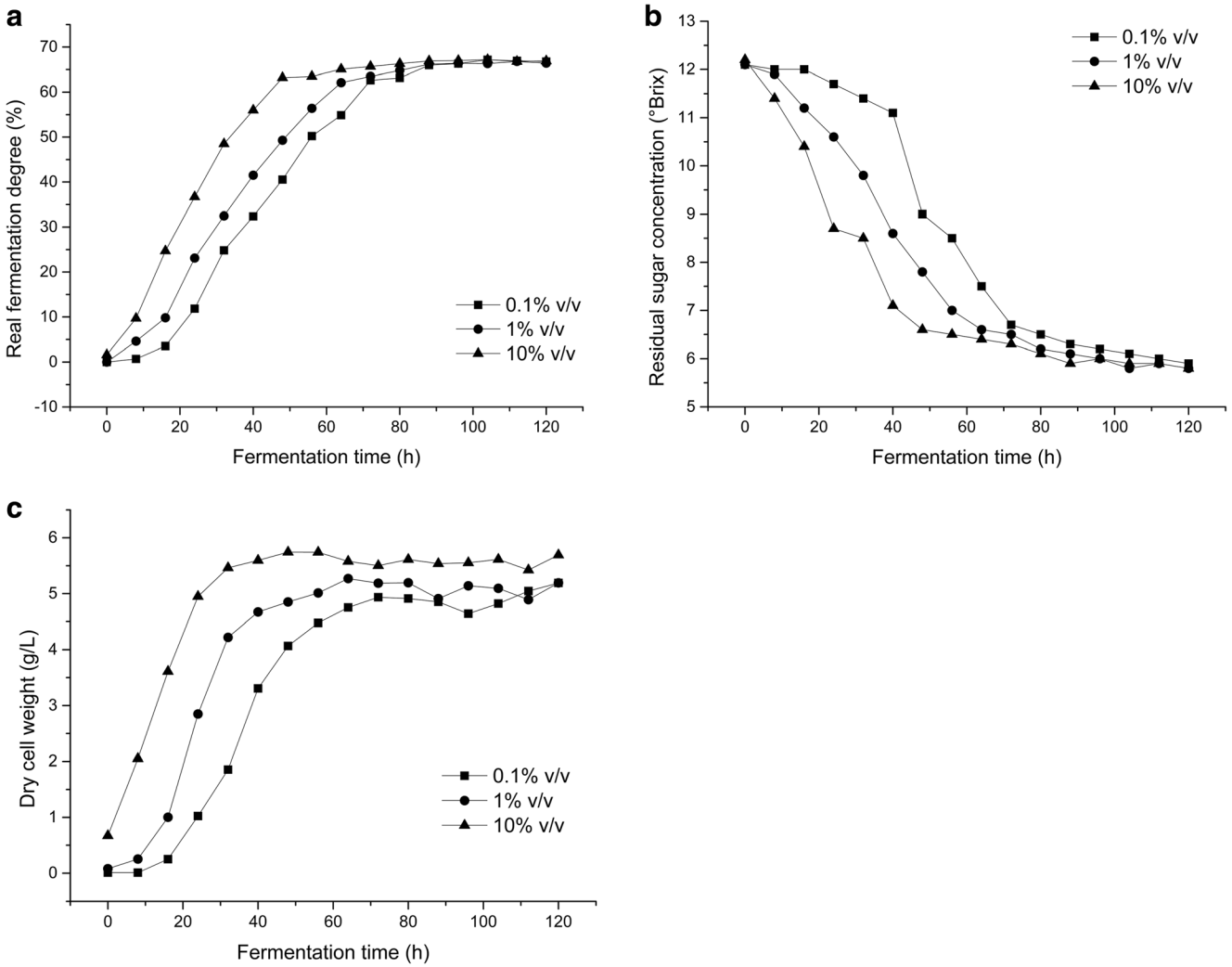

Fig. 1 Fermentation characteristics at different inoculum sizes (0.1% *v/v*, 1% *v/v*, 10% *v/v*). **a** Real fermentation degree at different inoculum sizes. **b** Residual sugar concentration at different inoculum sizes. **c** Growth curve of *S. cerevisiae* S-17 at different inoculum sizes

exponential growth phase when sufficient nutrients are not limiting.

Production of higher alcohols at three different inoculum sizes

The final concentrations of n-propanol, isobutanol, isoamylol, active amyl alcohol, and 2-phenylethanol produced by top-fermenting yeast *S-17* were decreased by 25.01%, 25.27%, 19.51%, 25.87%, and 22.24%, respectively, at the lowest inoculum size, compared to the normal pitching rate (Fig. 2), suggesting that the total concentration of higher alcohols decreases with decreasing pitching rate. Moreover, we virtually did not observe any higher alcohols produced during the initial stage of fermentation at the lower inoculum density, which can be explained by the cell growth in this phase.

Table 1 Kinetic parameters estimated from the experimental results at different inoculum sizes

Inoculum size	C_0 (g L^{-1})	C_m (g L^{-1})	u_m (h^{-1})	Adjusted *R*-square
0.1% *v/v*	0.0093	4.9343	0.17252	0.98923
1% *v/v*	0.0801	5.27001	0.16949	0.98784
10% *v/v*	0.67207	5.57898	0.17273	0.98797

Moreover, the accumulation of higher alcohols during the exponential growth phase (P_e) (mg/L), the accumulation of higher alcohols during the stationary phase (P_s) (mg/L), and the exponential growth phase (Y_e) (mg/g) and the stationary phase (Y_s) (mg/g) can be calculated as follows:

$$Pe = Pm - P0 \tag{6}$$

$$Ps = Pf - Pm \tag{7}$$

$$Ye = \frac{Pe}{Cm - C0} \tag{8}$$

$$Ys = \frac{Ps}{Cm} \tag{9}$$

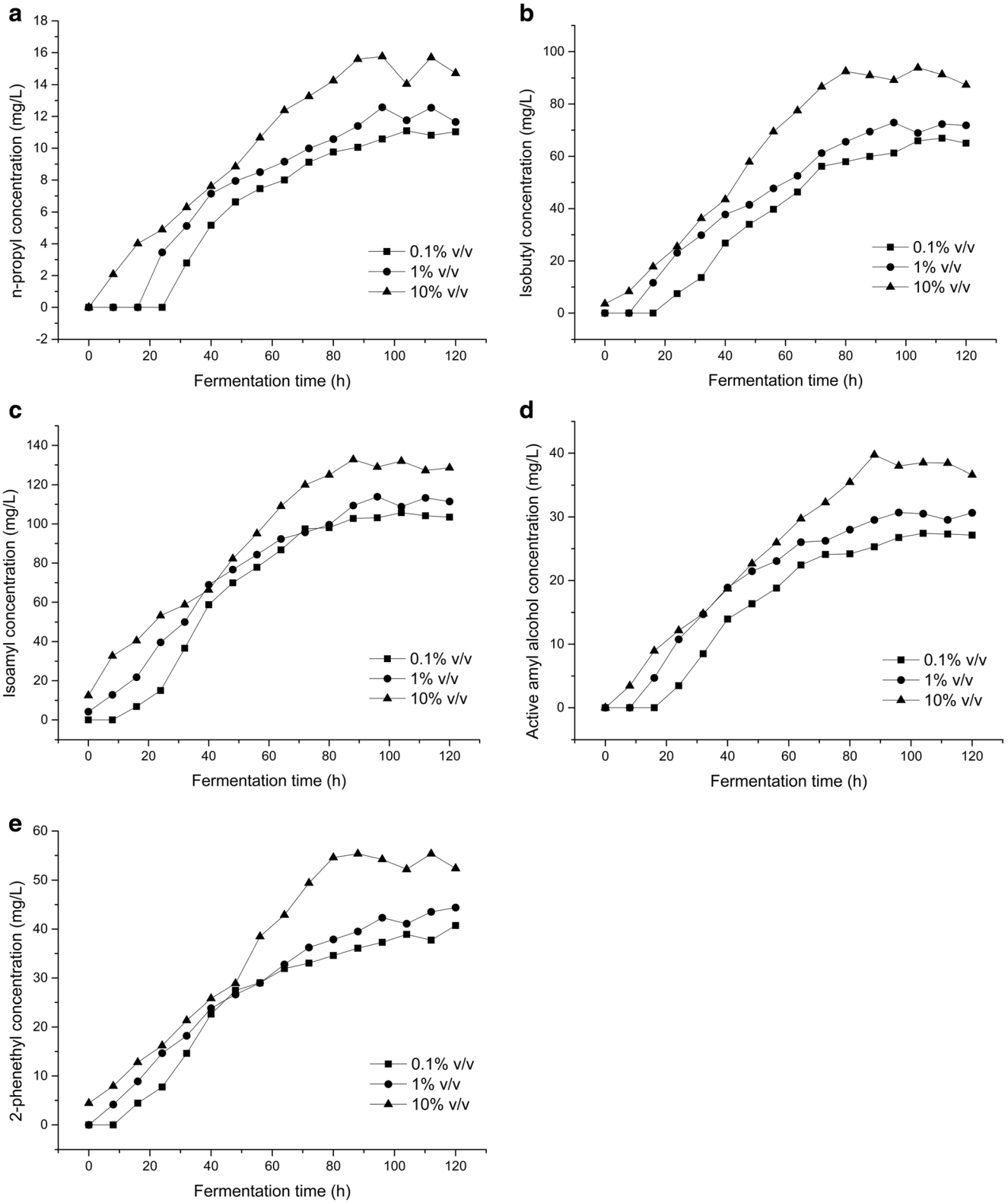

Fig. 2 Production curve of higher alcohols at different pitching rates (0.1% *v/v*, 1% *v/v*, 10% *v/v*). **a** N-propanol. **b** Isobutanol. **c** Isoamylol. **d** Active amyl alcohol. **e** 2-Phenylethanol

where P_0 is the production concentration when $C_x = C_0$ (mg/L), P_m is the production concentration when $C_x = C_m$ (mg/L), and P_f is the production concentration at the end of fermentation (mg/L) (Table 2).

As shown in Table 2, we did not observe any significant differences in n-propanol, isobutanol, or active amyl alcohol concentrations with decreasing pitching rates during the exponential growth phase, but slight increases were found for isoamylol and 2-phenylethanol alcohol. Moreover, the net growth of the yeast cell populations and the resulting accumulation of higher alcohols per biomass were not significantly different at different inoculum sizes during the exponential growth phase. In contrast, we observed significantly lower levels of n-propanol, isobutanol, isoamylol, active amyl alcohol, and 2-phenylethanol at lower cell inoculum density during the stationary phase, which is likely the most significant consequence of decreasing concentration of total higher alcohols with lower pitching rates. Specifically, the difference in the accumulation of higher alcohols during entire fermentation process was mainly reflected in the stationary phase. Overall, we can conclude that the production of higher alcohols is indirectly related to the rate of yeast cell growth.

Importantly, n-propanol, isobutanol, isoamylol, and active amyl alcohol, but not 2-phenylethanol, were predominantly produced during the exponential growth phase at the normal pitching rate. In *Saccharomyces cerevisiae*, 2-phenylethanol has been reported as one of the quorum-sensing molecules and its production is induced by cell density. Owing to these considerations, higher levels of 2-phenylethanol are seen in high cell density fermentation (Chen and Fink 2006; Wuster and Babu 2009; Avbelj et al. 2015).

Table 2 The accumulation of higher alcohols during the exponential growth phase (P_e) (mg/L) and the stationary phase (P_s) (mg/L)

Higher alcohols		0.1% *v/v*	1% *v/v*	10% *v/v*
n-propanol	P_e (mg/L)	9.1213	9.15672	8.84451
	P_s (mg/L)	1.97361	3.41549	6.74617
	Y_e (mg/g)	1.85242	1.76774	1.71035
	Y_s (mg/g)	0.39998	0.6481	1.17463
Isobutanol	P_e (mg/L)	56.14661	52.49686	54.28001
	P_s (mg/L)	9.77534	20.39663	34.61541
	Y_e (mg/g)	11.40264	10.13471	10.49668
	Y_s (mg/g)	1.9811	3.87032	6.02716
Isoamylol	P_e (mg/L)	97.46942	88.07545	69.79838
	P_s (mg/L)	8.27963	21.56957	50.47457
	Y_e (mg/g)	19.79476	17.00328	13.4976
	Y_s (mg/g)	1.68148	4.16408	9.76076
Active amyl alcohol	P_e (mg/L)	24.09954	26.02771	22.64125
	P_s (mg/L)	3.3164	4.66962	17.09771
	Y_e (mg/g)	4.8943	5.02474	4.37836
	Y_s (mg/g)	0.67352	0.90149	3.30635
2-Phenylethanol	P_e (mg/L)	33.03264	32.76246	24.42784
	P_s (mg/L)	5.88187	9.55504	26.46779
	Y_e (mg/g)	6.7085	6.32491	4.72385
	Y_s (mg/g)	1.19453	1.84463	5.69848

The accumulation of higher alcohols per unit cell during the exponential growth phase (Y_e) (mg/g) and the stationary phase (Y_s) (mg/g)

Kinetics of higher alcohol production

Data in Table 3, include parameters that were estimated from the experimental data using OriginPro (v9.0.0) software.

As shown in Table 3, the correlation coefficient (*R*-square) values for all models were between 0.97218 and 0.99536 at different inoculum densities, suggesting that the utilized equations accurately reflected the higher alcohol accumulation process in top-fermenting yeast S-17 during wheat beer fermentation. According to $\alpha \neq 0$, and $\beta \neq 0$, the data suggest that the total higher alcohol synthesis was partially related to yeast cell growth. Moreover, the values of the growth-associated constant (α) divided by the non-growth associated constant (β) were significantly increased in all of higher alcohols at the lowest inoculum size. Overall, our data suggest that the correlation between higher alcohol synthesis and yeast cell growth is negatively regulated by the inoculum size during the fermentation process. Additionally, we also demonstrated that the proportion of higher alcohols formed by resting yeast cells decreased with decreasing pitching rates. In accordance with earlier findings, we observed significantly less of higher alcohols at the lower cell inoculum density during the stationary phase. Therefore, we hypothesized that the ability of yeast to synthesize higher alcohols during the stationary phase was reduced at lower inoculum sizes.

To assess the ability of yeast cells to synthesize higher alcohols during the stationary phase at decreasing and normal pitching rates, we examined FAN consumption and AP.

FAN consumption

We observed that the final FAN consumption was decreased by approximately 18% at the lowest pitching rate, suggesting a direct relationship between these two parameters (Fig. 3). In addition, there were no significant differences in the amount of FAN consumption during the exponential growth phase at the decreasing pitching rates. The concentration of FAN consumption during the stationary phase was drastically decreased between the normal pitching rate (37.05803 mg/L) and the lowest pitching rate (1.92808 mg/L). Based on these data, we hypothesized that the ability of the top-fermenting yeast to synthesize higher alcohols via the catabolic (Ehrlich) pathway was significantly reduced with decreasing pitching rates during the stationary phase.

AP test

The test provides a fast and effective method of assessing yeast cell viability, and it was first designed by Opekarová and Sigler in 1982 (Opekarová and Sigler 1982; Gabriel

Table 3 Kinetic parameters estimated from the experimental results at different inoculum sizes

Higher alcohols	Kinetic parameters	0.1% *v/v*	1% *v/v*	10% *v/v*
n-propanol	α	1.31507	1.06797	1.04123
	β	0.01384	0.01765	0.03366
	Adjusted *R*-square	0.99451	0.9903	0.97218
Isobutanol	α	6.81239	5.8484	2.46548
	β	0.09982	0.11311	0.23433
	Adjusted *R*-square	0.99174	0.98876	0.98938
Isoamylol	α	15.65305	10.58659	7.98934
	β	0.08949	0.14555	0.26384
	Adjusted *R*-square	0.9882	0.992	0.97383
Active amyl alcohol	α	3.63225	3.31631	2.18793
	β	0.02905	0.03597	0.08578
	Adjusted *R*-square	0.9906	0.99536	0.97655
2-Phenylethanol	α	6.0125	4.01302	1.46117
	β	0.02437	0.05582	0.12048
	Adjusted *R*-square	0.97644	0.98024	0.98851

et al. 2012). The AP test requires two values were calculated: the glucose acidification power (GAP) and glucose-induced proton efflux (GIPE). GAP represents the change in pH once yeast cells are resuspended in water for 10 min followed by 10 min in glucose, while GIPE is the change in, pH between 20 and 10 min, which represents the ability of yeast cells to use extracellular reserves, without taking into account the utilization of intracellular reserves (Kara et al. 1988; Rotar and Stoicescu 2006).

As shown in Fig. 4, the values of GAP and GIPE exhibited small changes within 24 h, indicating that the yeast cells remained active and were capable of producing higher alcohols within this time. Importantly, both GAP and GIPE were significantly decreased after 36 h, suggesting that the majority of cells were in the declining phase and virtually no higher alcohols were synthesized within that time frame. Importantly, we also observed significant decreases in GAP and GIPE values at the lowest inoculum density, suggesting a decrease in yeast cell viability at lower inoculum sizes during the stationary phase. Overall, these results suggest that the ability of yeast to synthesize higher alcohols during the stationary phase is reduced with decreasing pitching rates.

Transcriptional responses

Data presented in Table 4 show a comparison of the gene transcript levels between the normal pitching rate (10% *v/v*) and the lower pitching rate (0.1% *v/v*) at the declining growth phase to uniquely responsive transcripts at each inoculum size. We used DESeq2 software for the statistical analysis of the data used a minimum fold change cutoff of 2. The false discovery rate (FDR = percentage of called genes that are expected to be false positives) was set to 1%. Compared with the normal inoculum size, we identified 36 significant differentially expressed genes, of which 3 were induced and were suppressed at the lowest pitching rate. As shown in Fig. 5 and Table 5, we mapped 15 unigenes to 25 pathways in the KEGG database to assess the significance and biological function of the differentially transcribed genes.

The most significantly enriched pathways were related to amino acid metabolism, including branched-chain amino acids, alanine, histidine, lysine, aromatic amino acid, arginine, and proline. The dgenes *ALD4* and *ALD6*, involved inthemetabolic pathway of branched chain amino acids, histidine, lysine, arginine, and proline, were significantly suppressed at the lowest pitching rate.

Discussion

Lower pitching rates result in lower levels of higher alcohols, although the alcohol concentration, sugar consumption, and Rdf exert no significant effects at different inoculum sizes. Studies comprehensively examining these parameters can provide a potential advantage for improving the quality of wheat beer. One of the main and significant problems associated with the fermentation at low pitching rates is extended fermentation time. We observed that the lowest inoculum density (0.1% *v/v*) was associated with an initial adaptation phase prior to the exponential growth. This can likely be explained by the fact that certain growth factors and signaling molecules released by yeast cells did not reach appropriate concentrations given the low initial number of cells which were diluted into a new fresh culture, a very typical quorum-sensing

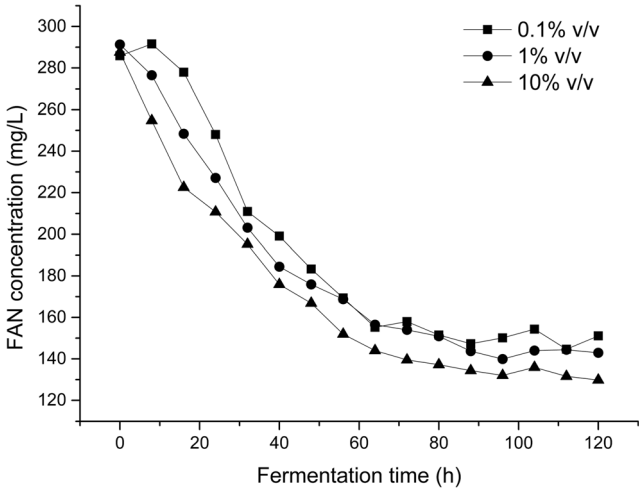

Fig. 3 Free amino nitrogen (FAN) consumption with lowest pitching rate (0.1% *v*/*v*) and normal pitching rate (10% *v*/*v*)

behavior, where the lower the initial concentration of cells is, the longer it takes for cells to enter into exponential growth (Chen et al. 2004). Potentially, this could also serve as an explanation for extended fermentation times at the lower inoculum sizes. They suggested that this phenomenon could be abolished by using conditioned medium in *Candida albicans*. Therefore, additional studies examining the correlation between the pitching rate and quorum-sensing behaviors in *Saccharomyces cerevisiae* are warranted.

In this paper, we proposed a nonlinear kinetic model for wheat beer fermentation by a top-fermenting yeast S-17 at different inoculum sizes, which incorporates the logistic equation of cell growth and Luedeking-Piret equation of higher alcohol synthesis. In our calculations, some kinetic parameters were estimated by the mathematical software, which could be used for predicting wheat beer fermentation performance at different inoculum densities. Our results indicated that growth-associated constant is increased and non-growth associated constant is decreased at lower pitching rates. It is widely accepted that higher alcohols are formed by growing cells and resting cells (Ingraham and Guymon 1960; Bevers and Verachtert 1976). Therefore, we demonstrated that the proportion of higher alcohols formed by resting yeast cells decreased with decreasing pitching rates. Additionally, we observed that significantly lower levels of higher alcohols were produced at lower cell inoculum density during the stationary phase, indicating that the difference in the accumulation of higher alcohols during the entire fermentation process is mainly reflected in the stationary phase.

The synthesis of higher alcohols is directly related to the uptake level of amino acids. The results presented herein demonstrate that the concentration of FAN consumption during the stationary phase was significantly reduced with decreasing pitching rate. Also, we noted that the yeast cell viability was decreased with lower pitching rates during the stationary phase. We can therefore conclude that the ability of yeast to synthesize higher alcohols was reduced with decreasing pitching rate. Previous study has found that the high-density fermentation was linked with a percentage of aged cells, possibly due to the depletion of oxygen (Edelen et al. 1996). Aged cells have been shown to ferment more efficiently and at a higher rate than mixed aged or virgin cell cultures (Powell et al. 2003). Overall, these finding can likely explain the difference in performance between the normal pitching rate and lower pitching rate during the stationary phase.

Transcriptome analysis revealed that amino acid metabolism was significantly affected, in agreement with significant expression of differentially transcribed genes *ALD4*, *ALD6*, *ARO9*, *ARO10*, and *PUT1* once the cells entered the declining growth phase at the lowest cell inoculum size.

The *ALD4* and *ALD6* genes in *S. cerevisiae* have been reported to encode mitochondrial aldehyde dehydrogenase

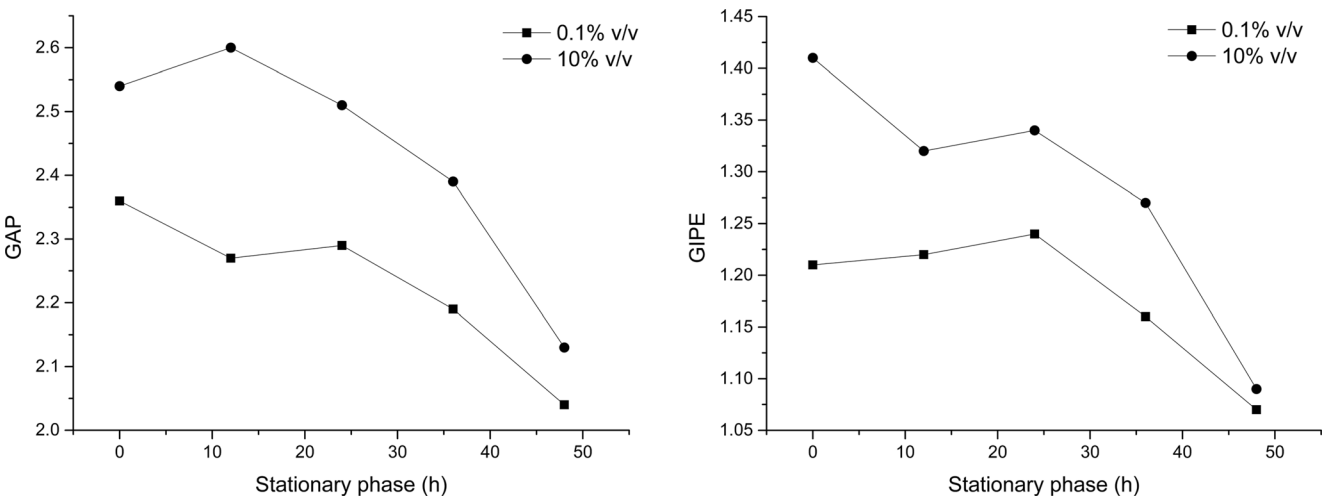

Fig. 4 The acidification test with lowest pitching rate (0.1% *v*/*v*) and normal pitching rate (10% *v*/*v*) during the stationary phase (0 to 50 h). **a** Glucose acidification power (GAP) curve. **b** Glucose-induced proton efflux (GIPE) curve

Table 4 Differential gene expression of transcripts by at least two-fold in the lowest pitching rate (0.1% *v/v*) compared to the normal pitching rate (10% *v/v*)

Gene/ORF	Definition	Regulation	baseMeanA	baseMeanB	Fold change
SUT1	Sucrose transport protein	Down	1227.851556	567.8015366	0.462435002
PDR15	ATP-binding cassette multidrug transporter ATP	Down	16,331.49508	7263.127989	0.444731358
DAL80	GATA-binding protein, other eukaryote GATA	Down	933.2838427	356.9332123	0.382448721
ALD4	Aldehyde dehydrogenase (NAD^+)	Down	12,065.61018	4724.47909	0.3915657
ALD6	Aldehyde dehydrogenase (NAD^+)	Down	23,908.59328	4823.227183	0.201736134
PUT4	Yeast amino acid transporter	Down	3179.97026	653.1774923	0.205403648
UGA4	GABA-specific permease	Down	1987.116848	957.65078	0.481929777
MEP1	Ammonium transporter, Amt family	Down	2578.196616	1227.150785	0.475972537
ARO10	Phenylpyruvate decarboxylase	Down	3267.46562	1156.175593	0.353844761
ARO9	Aromatic amino acid aminotransferase II	Down	2059.057478	509.1698562	0.247282974
MPC3	Mitochondrial pyruvate carrier	Down	1106.330222	374.4198539	0.338434083
FMP48	Protein-serine/threonine kinase	Down	2219.465639	837.3015413	0.377253663
MKK1	Mitogen-activated protein kinase kinase	Ups	530.8051856	1195.26338	2.251792959
RCK1	Protein-serine/threonine kinase	Down	279.0129822	115.2061089	0.412905908
FLO11	Glucoamylase	Ups	153.6029658	381.6202357	2.484458771
IMA2	Alpha-glucosidase	Down	772.8756823	244.8129814	0.316755963
IMA5	Alpha-glucosidase	Down	315.9554676	127.5496205	0.403694931
GPT2	Glycerol-3-phosphate O-acyltransferase /dihydroxyacetone phosphate acyltransferase	Down	2313.766193	919.5916191	0.397443623
HXT2	MFS transporter, SP family, sugar:H+ symporter hexose transporter	Down	5452.905285	2064.452326	0.37859677
HXT4	MFS transporter, SP family, sugar:H+ symporter	Ups	284.8460062	580.1450483	2.036697148
DAL4	Nucleobase:cation symporter-1, NCS1 family	Down	1849.068613	606.8893235	0.328213523
PUT1	Proline dehydrogenase	Down	4339.769869	1387.616436	0.319744244
ADY2	Accumulation of dyad protein 2	Down	242.0704967	52.45992458	0.216713417
PHM7	Phosphate metabolism protein 7	Down	825.3728984	334.3034409	0.405033218
DAL2	Allantoicase	Down	1779.072325	835.2442894	0.469483043
DAL3	Ureido glycolate hydrolase	Down	625.1057405	236.5839736	0.378470326
CIN5	AP-1-like transcription factor	Down	598.8571324	170.7519114	0.285129628
CWP1	Cell wall protein	Down	1719.769914	719.0095545	0.418084738
PNS1	Protein PNS1	Down	2725.966557	1097.543912	0.402625597
NCE103	Carbonic anhydrase	Down	2228.215175	823.9294037	0.369771023
BAG7	BAG family molecular chaperone regulator 7	Down	1773.239301	801.2996323	0.451884656
XBP1	Transcriptional repressor XBP1	Down	626.0779112	217.0400801	0.346666248
YBR126W-A	Hypothetical protein	Down	654.2708606	236.5839736	0.361599435
YJR115W	Hypothetical protein	Down	1077.165102	510.1984822	0.473649287
YNR014W	Hypothetical protein	Down	577.4693777	288.0152722	0.498754191
YPR145C-A	Hypothetical protein	Down	838.9832878	401.1641291	0.47815509

and cytosolic aldehyde dehydrogenase, respectively, which are required for the conversion of fusel aldehydes to fusel acids. Work by Hazelwood et al. suggested that oxidation of isobutyraldehyde to isobutyrate by aldehyde dehydrogenases (*ALDs*) competes with the production of isobutanol (Horton et al. 2003; Saintprix et al. 2004; Hazelwood et al. 2008) and isoamyl and isobutyraldehyde are known to be oxidized into corresponding acids by aldehyde dehydrogenases (*ALDs*) (Pank et al. 2014). *ALD4* and *ALD6* have been shown to be involved in the pyruvate metabolism by converting aldehyde to acetate, which can also help explain the formation of higher alcohols by top-fermenting yeast.

Based on the sequencing data, we discovered that the aromatic amino acid (phenylalanine, tyrosine, and tryptophan) metabolism was likely weakened by suppression of *ARO9* and *ARO10* genes at the lowest inoculum size. *ARO9p* and *ARO10p* were characterized as the aromatic amino acid aminotransferase and transaminated amino acid decarboxylase, respectively. Specifically, *ARO9p* catalyzes the first step (the transamination step) of

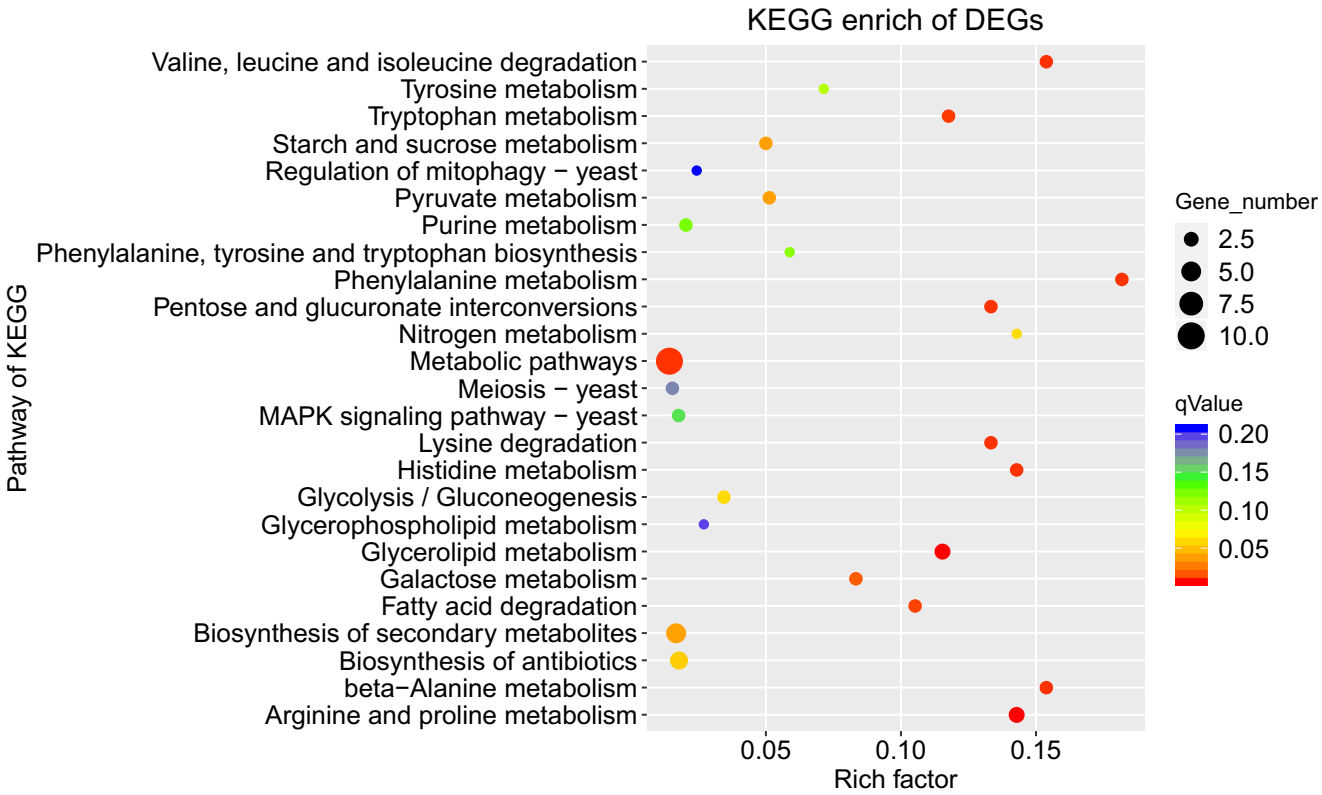

Fig. 5 Scatter plot of unigenes mapped to the KEGG database. The horizontal coordinate represents the pathway name and the vertical coordinate represents the Rich factor, where the greater the value of Rich factor is, the greater the degree of enrichment is. The range of qValue is between 0 and 1, with values closer to zero showing greater enrichment

phenylalanine, tyrosine, and tryptophan catabolism in *S. cerevisiae*, while *ARO10p* protein carries out the decarboxylation of phenypyruvate to 2-phenylacetaldehyde. Studies show that *ARO9p* and *ARO10p* are also involved in branched-chain amino acid metabolism, suggesting that they have a broad substrate-specific activity and can strongly affect the formation of higher alcohols (Urrestarazu et al. 1998; Li et al. 2017). In addition, the aromatic alcohols phenylethanol and trytophol have been shown to be quorum-sensing molecules in *S. cerevisiae*, which are induced by cell density. Importantly, high levels of these quorum-sensing molecules induce the expression of *ARO9* and *ARO10* genes, in turn stimulating the accumulation of aromatic alcohols and creating a positive feedback loop (Chen and Fink 2006; Wuster and Babu 2009; Avbelj et al. 2015). This could likely explain the relatively low expression of *ARO9* and *ARO10* in the cells entering the declining growth phase at the lowest cell inoculum size.

Branched chain amino acids and aromatic amino acids are directly linked with the synthesis of higher alcohols. High cell concentration was linked with the induction of *ARO9* and *ARO10* genes and, thus, likely affected the formation of higher alcohols, which can explain the lower expression of *ARO9* and *ARO10* once the cells entered the declining growth phase at the lowest cell inoculum size. However, additional studies are required to fully elucidate the mechanism underlying the variable pitching rate effects on the expression of other differentially transcribed genes.

Furthermore, we observed changes in the expression of *PUT1* (proline dehydrogenase), suggesting that the metabolism of proline was also significantly affected by pitching rate. Importantly, studies suggest that proline is a significant amino acid that affects the production of higher alcohols in *S. cerevisiae* (Procopio et al. 2011). Moreover, nitrogen metabolism was also weakened at the lowest cell inoculum size, which may help explain the formation of higher alcohols and the lower FAN consumption.

This work provides significant evidence that the yeast cell viability was reduced at lower inoculum sizes when cell growth entered the stationary phase. This will likely have a negative impact on the synthesis of higher alcohols during the stationary phase and ultimately lead to the decreased levels of higher alcohols at the lower inoculum sizes. Moreover, we demonstrated that the transcriptional changes were significantly affected by pitching rate at the declining growth phase, and therefore likely affected the amino acid metabolism and formation of higher alcohols. Finally, the properties of enzymes or proteins involved in the higher alcohol metabolism should be given additional attention and should be further

Table 5 Kyoto Encyclopedia of Genes and Genomes (KEGG) enrichment analysis under different pitching rates

KEGG pathway	Gene	Input number	Background number	*P* value	qValue	Rich factor
Valine, leucine, and isoleucine degradation	*ALD4/ALD6*	2	13	0.002947298	0.010531173	0.153846154
Beta-alanine metabolism	*ALD4/ALD6*	2	13	0.002947298	0.010531173	0.153846154
Histidine metabolism	*ALD4/ALD6*	2	14	0.003356747	0.010531173	0.142857143
Lysine degradation	*ALD4/ALD6*	2	15	0.003791222	0.010531173	0.133333333
Pentose and glucuronate interconversions	*ALD4/ALD6*	2	15	0.003791222	0.010531173	0.133333333
Tryptophan metabolism	*ALD4/ALD6*	2	17	0.004734172	0.011835429	0.117647059
Fatty acid degradation	*ALD4/ALD6*	2	19	0.005773998	0.013122724	0.105263158
Pyruvate metabolism	*ALD4/ALD6*	2	39	0.021051103	0.039336123	0.051282051
Glycolysis/gluconeogenesis	*ALD4/ALD6*	2	58	0.042590703	0.059948842	0.034482759
Arginine and proline metabolism	*ALD4/ALD6/PUT1*	3	21	0.000284614	0.006302967	0.142857143
Glycerolipid metabolism	*GPT2/ALD4/ALD6*	3	26	0.000504237	0.006302967	0.115384615
Biosynthesis of secondary metabolites	*ALD4/ALD6/PUT1/GPT2/APR9*	5	298	0.02371846	0.039530767	0.016778523
Biosynthesis of antibiotics	*ALD4/ALD6/PUT1/ARO9*	4	224	0.035164166	0.05494401	0.017857143
Phenylalanine metabolism	*ARO9/ARO10*	2	11	0.002204579	0.010531173	0.181818182
Tyrosine metabolism	*ARO9*	1	14	0.079441916	0.104528836	0.071428571
Phenylalanine, tyrosine, and tryptophan biosynthesis	*ARO9*	1	17	0.094577626	0.118222033	0.058823529
Nitrogen metabolism	*NCE103*	1	7	0.043163166	0.059948842	0.142857143
Galactose metabolism	*IMA2/IMA5*	2	24	0.00878361	0.018299187	0.083333333
Starch and sucrose metabolism	*IMA2/IMA5*	2	40	0.022028229	0.039336123	0.05
Purine metabolism	*DAL2/DAL3*	2	98	0.104080069	0.123904844	0.020408163
MAPK signaling pathway—yeast	*FLO11/MKK1*	2	113	0.131096838	0.14897368	0.017699115
Meiosis—yeast	*HXT4/HXT2*	2	130	0.163435222	0.177646981	0.015384615
Glycerophospholipid metabolism	*GPT2*	1	37	0.189479433	0.197374409	0.027027027
Regulation of mitophagy—yeast	*MKK1*	1	41	0.207264475	0.207264475	0.024390244
Metabolic pathways	*DAL2/PUT1/ARO9/IMA2/ALD4/ALD6/IMA5/GPT2/DAL3/ARO10*	10	699	0.003766917	0.010531173	0.014306152

examined under different pitching rates, to ultimately help unravel the regulatory mechanisms of higher alcohol metabolites.

Funding This work was supported by the National Natural Science Foundation of China (No. 31771969), the National Key Research and Development Program of China (No. 2016YFD0400505), the China Postdoctoral Science Foundation (2017M611169), the Hebei Province Postdoctoral Research Projects (No. B2018003031) and the Public Service Platform Project for Selection and Fermentation Technology of Industrial Microorganisms (No. 17PTGCCX00190).

Compliance with ethical standards

Conflict of interest The authors declare that they have no conflict of interest.

Research involving human participants and/or animals This article does not contain any studies with human participants or animals performed by any of the authors.

References

Avbelj M, Zupan J, Kranjc L, Raspor P (2015) Quorum-sensing kinetics in *Saccharomyces cerevisiae*: a symphonyof *ARO* genes and aromatic alcohols. J Agric Food Chem 63:8544–8550

Bevers J, Verachtert H (1976) Synthesis of higher alcohols in the genus zymomonas. J Inst Brew 82:35–40

Carrau F, Medina K, Fariña L, Boido E, Dellacassa E (2010) Effect of *Saccharomyces cerevisiae* inoculum size on wine fermentation aroma compounds and its relation with assimilable nitrogen content. Int J Food Microbiol 143:81–85

Chen EH (1978) Effects on flavour of innovations in brewery equipment and processing: a review. J Inst Brew 107:271–286

Chen H, Fink GR (2006) Feedback control of morphogenesisin fungi by aromatic alcohols. Genes Dev 20:1150–1161

Chen H, Fujita M, Feng Q, Clardy J, Fink GR (2004) Tyrosol is a quorum-sensing molecule in *Candida albicans*. Proc Natl Acad Sci USA 101:5048–5052

Edelen CL, Miller JL, Patino H (1996) Effects of yeast pitching rates on fermentation performance and beer quality. Tech Q Master Brew Assoc Am 33:30–32

Engan S (1981) In: Pollock JRA (ed) Brewing science, vol. Academic Press, London, p 2

Erten H, Tanguler H, Cakiroz H (2007) The effect of pitchinging rate on fermentation and flavour compounds in high gravity brewing. J Inst Brew 113:75–79

European Brewery Convention (1998) Analytica–EBC. Fachverlag Hans Carl, Nürnberg

Gabriel P, Dienstbier M, Matoulková D, Kosař K, Sigler K (2012) Optimised acidification power test of yeast vitality and its use in brewing practice. J Inst Brew 114:270–276

Hammond JRM (1993) In: Rose AH, Harrison JS (eds) The yeasts, vol 5: yeast technology. Academic Press, London

Hazelwood L, Daran J, Van Maris A et al (2008) The Ehrlich pathway for fusel alcohol production: a century of research on *Saccharomyces cerevisiae* metabolism. Appl Environ Microbiol 74:2259–2266

Horton CE, Huang KX, Bennett GN, Rudolph FB (2003) Heterologous expression of the *Saccharomyces cerevisiae* alcohol acetyltransferase genes in *Clostridium acetobutylicum* and *Escherichia coli* for the production of isoamyl acetate. J Ind Microbiol Biotechnol 30:427–432

Huang C, Li YY, Liu LP, Wu H et al (2014) Kinetics and mechanism analysis on microbial oil production by *Trichosporon fermentans* in rice straw hydrolysate. Ind Eng Chem Res 53:19034–19043

Ingraham JL, Guymon JF (1960) The formation of higher alcohols by mutant strains of *Saccharomyces cerevisiae*. Arch Biochem Biophys 88:157–166

Kara BV, Simpson WJ, Hammond JRM (1988) Prediction of the fermentation performance of brewing yeast with the acidification power test. J Inst Brew 94:153–158

Kim D, Langmead B, Salzberg SL (2015) HISAT: a fast spliced aligner with low memory requirements. Nat Methods 12:357–360

Kobayashi M, Nagahisa K, Shimizu H, Shioya S (2014) Simultaneous control of apparent extract and volatile compounds concentrations in low-malt beer fermentation. Appl Microbiol Biotechnol 73:549–558

Kumar S, Dheeran P, Singh SP, Mishra IM, Adhikari DK (2014) Kinetic studies of ethanol fermentation using *Kluyveromyces* sp. IIPE453. J Chem Technol Biotechnol 88:1874–1884

Landaud S, Latrille E, Corrieu G (2001) Top pressure and temperature control the fusel alcohol/Ester ratio through yeast growth in beer fermentation. J Inst Brew 107:107–117

Li J, Feng R, Wen Z, Zhang A (2017) Overexpression of *ARO10* in pdc5ΔMutant resulted in higher isobutanol titers in *Saccharomyces cerevisiae*. Biotechnol Bioprocess Eng 22:382–389

Luedeking R, Piret EL (1959) A kinetic study of the lactic acid fermentation. Batch process at controlled pH. J Biochem Microbiol Technol Eng 4:393–412

Ma LJ, Huang SY, Du LP, Tang P, Xiao DG (2017) Reduced production of higher alcohols by *Saccharomyces cerevisiae* in red wine fermentation by simultaneously overexpressing *BAT1* and deleting *BAT2*. J Agric Food Chem 65:6936–6942

Meilgaard MC (1975) Flavor chemistry of beer: part II: flavor threshold of 239 aroma volatiles. Tech Q Master Brew Assoc Am 12:151–168

Meilgaard MC (2001) Effects on flavour of innovations in brewery equipment and processing: a review. J Inst Brew 107:271–286

Okabe M, Katoh M, Furugoori F, Yoshida M, Mitsui S (1992) Growth and fermentation characteristics of bottom brewer's yeast under mechanical stirring. J Ferment Bioeng 73:148–152

Opekarová M, Sigler K (1982) Acidification power: Indicator of metabolic activity and autolytic changes in *Saccharomyces cerevisiae*. Folia Microbiol 27:395–403

Pank SH, Kim S, Hahn JS (2014) Metabolic engineering of *Saccharomyces cerevisiae* for the production of isobutanol and 3-methyl-1-butanol. Appl Microbiol Biotechnol 98:9139–9147

Pires EJ, Teixeira JA, Branyik T, Vicente AA (2014) Yeast: the soul of beer's aroma—a review of flavour-active esters and higher alcohols produced by the brewing yeast. Appl Microbiol Biotechnol 98: 1937–1949

Powell CD, Quain DE, Smart KA (2003) Quain DE and Smart KA, The impact of brewing yeast cell age on fermentation performance, attenuation and flocculation. FEMS Yeast Res 3:149–157

Procopio S, Qian F, Becker T (2011) Function and regulation of yeast genes involved in higher alcohol and ester metabolism during beverage fermentation. Eur Food Res Technol 233:721–729

Rotar R, Stoicescu AG (2006) Modified acidification power test applied to evaluate temperature and ethanol stress impact on yeast fermentation performance. J Agroaliment Process Technol 2:481–488

Saerens SM, Verbelen PJ, Vanbeneden N, Thevelein JM, Delvaux FR (2008) Monitoring the influence of high-gravity brewing and fermentation temperature on flavour formation by analysis of gene expression levels in brewing yeast. Appl Microbiol Biotechnol 80: 1039–1051

Saintprix F, Bönquist L, Dequin S (2004) Functional analysis of the *ALD* gene family of *Saccharomyces cerevisiae* during anaerobic growth on glucose: the $NADP^+$-dependent *Ald6p* and *Ald5p* isoforms play a major role in acetate formation. Microbiology 150:2209–2220

Sen R, Swaminathan T (2004) Response surface modeling and optimization to elucidate and analyze the effects of inoculum age and size on surfactin production. Biochem Eng J 21:141–148

Urrestarazu A, Vissers S, Iraqui I, Grenson M (1998) Phenylalanine and tyrosine-auxotrophic mutants of *Saccharomyces cerevisiae* impaired in transamination. Mol Gen Genet 257:230–237

Vanderhaegen B, Neven H, Coghe S, Verstrepen KJ, Verachtert H, Derdelinckx G (2003) Evolution of chemical and sensory properties during aging of top-fermented beer. J Agric Food Chem 51:6782–6790

Verbelen PJ, Mulders SV, Saison D, Laere SV, Delvaux et al (2008) Characteristics of high cell density fermentations with different lager yeast strains. J Inst Brew 114:127–133

Verbelen PJ, Dekoninck TM, Saerens SM, Van Mulders SE, Thevelein JM et al (2009) Impact of pitchinging rate on yeast fermentation performance and beer flavour. Appl Microbiol Biotechnol 82:155–167

Wang D, Xu Y, Hu J, Zhao G (2015) Fermentation kinetics of different sugars by apple wine yeast *Saccharomyces cerevisiae*. J Inst Brew 110:340–346

Wuster A, Babu MM (2009) Transcriptional control of the quorum sensing response in yeast. Mol BioSyst 6:134–141

Zhang CY, Liu YL, Qi YN, Zhang JW, Dai LH (2013) Increased esters and decreased higher alcohols production by engineered brewer's yeast strains. Eur Food Res Technol 236:1009–1014